# Narrow-linewidth quantum cascade laser at 8.6 μm

**Eugenio Fasci,[1] Nicola Coluccelli,[2] Marco Cassinerio,[2] Alessio Gambetta,[2] Laurent Hilico,[3,4] Livio Gianfrani,[1] Paolo Laporta,[2] Antonio Castrillo,[1] and Gianluca Galzerano[2,*]**

[1]*Dipartimento di Matematica e Fisica, Seconda Università di Napoli, Viale Lincoln 5, 81100 Caserta, Italy*

[2]*Istituto di Fotonica e Nanotecnologie, CNR and Dipartimento di Fisica, Politecnico di Milano, Piazza Leonardo da Vinci 32, 20133 Milano, Italy*

[3]*Laboratoire Kastler Brossel, UEVE, Bd. F. Mitterrand, 91025 Evry, France*

[4]*UPMC, CNRS, ENS, 4 place Jussieu 75252 Paris, France*

**Corresponding author: gianluca.galzerano@polimi.it*

Received June 10, 2014; revised July 22, 2014; accepted July 22, 2014; posted July 24, 2014 (Doc. ID 213790); published August 15, 2014

We report on a narrow-linewidth distributed-feedback quantum cascade laser at 8.6 μm that is optical-feedback locked to a high-finesse V-shaped cavity. The spectral purity of the quantum cascade laser is fully characterized using a high-sensitivity optical frequency discriminator, leading to a 1 ms linewidth of less than 4 kHz and a minimum laser frequency noise spectral density as low as 0.01 $Hz^2/Hz$ for Fourier frequencies larger than 100 kHz. The cumulative standard deviation of the laser intensity is better than 0.1% over an integration bandwidth from 2 Hz to 100 MHz. 

*OCIS codes:* (140.3425) Laser stabilization; (140.5965) Semiconductor lasers, quantum cascade.
http://dx.doi.org/10.1364/OL.39.004946

Quantum cascade lasers (QCLs), in particular room-temperature distributed-feedback (DFB) lasers, are becoming the usual sources for accessing the mid-IR molecular fingerprint spectral region. For advanced applications in precision spectroscopy, much effort is aimed at further improving their spectral purity performance. Indeed, although the intrinsic emission linewidth of a QCL can be as low as a few hundred hertz [1,2], excess technical noise, such as the pump current noise, and internally induced QCL structure noise [3], broadens the QCL emission linewidth by several orders of magnitude up to few megahertz for 1 ms observation times. For this reason, different electronic feedback techniques have been implemented to narrow the QCL linewidth down to the 10 kHz level, such as locking to the side of a molecular line [4], to an optical cavity [5], and phase locking to a thulium frequency comb [6]. Even better results have been recently obtained using electronic feedback from a molecular sub-Doppler reference [7] and electronic phase locking to a $CO_2$ laser stabilized on a saturated absorption line of $OsO_4$ [8,9].

In this Letter, we demonstrate a high spectral purity room-temperature DFB-QCL tunable in the range from 8.56 to 8.63 μm. The QCL is phase locked to a high-finesse V-shaped cavity by the optical-feedback (OF) method [10–15]. This simple and robust technique narrows the 1 ms QCL linewidth from 3.2 MHz to 4 kHz. The OF-QCL is characterized in terms of both intensity and frequency noises. In particular, the frequency noise power spectral density (PSD) of the QCL is measured by using two different optical frequency discriminators based on the side of an absorption line of the $N_2O$ molecule and on a fringe side of a high-finesse Fabry–Perot (FP) resonator. In this way, both the free-running and the OF-locked operation of the QCL have been characterized with a limit frequency noise sensitivity as low as 0.01 $Hz^2/Hz$. This narrow-linewidth QCL source is a powerful tool for high-resolution molecular spectroscopy and optical frequency standard in the mid-IR spectral region. In particular, it will be used for the absolute measurement of the line center frequency of a two-photon transition in a $CHF_3$ molecular beam, allowing for a determination of a possible variation of the electron-to-proton mass ratio at a level of $10^{-15}$ $yr^{-1}$ [16].

The experimental layout is shown in Fig. 1. The OF-QCL configuration is similar to the one described in [17]. The locking technique exploits the OF coming from a high-finesse V-shaped cavity into the laser source. The V-shaped geometry allows only the intracavity radiation to feedback to the laser, avoiding direct backreflections from the input folding mirror, which would be detrimental for the laser emission spectrum. The DFB-QCL (Alpes Laser) operates at room temperature in a CW single mode at around 8.6 μm, with a maximum output power of 50 mW and a sidemode suppression of ~30 dB. CW tunability in the range from 8.56 to 8.63 μm can be obtained by a proper combination of laser temperature ($\Delta\nu/\Delta T = -0.086$ $cm^{-1}$ $K^{-1}$) and pump current ($\Delta\nu/\Delta I = -0.011$ $cm^{-1}/mA$) adjustments. Active control of the laser temperature with stability of few millikelvin over more

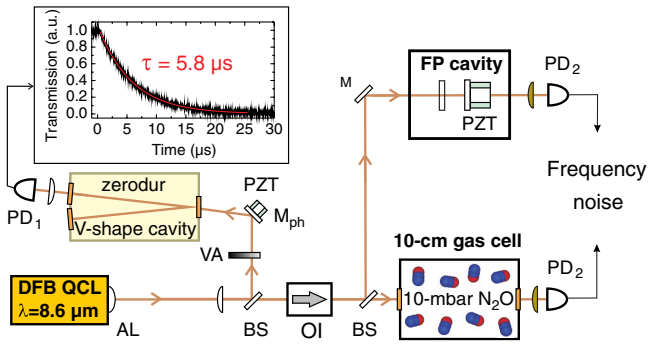


Fig. 1. Experimental setup for the OF of the QCL to a V-shaped cavity and for its characterization using optical frequency discriminators. AL, aspherical lens; BS, beam splitter; M, mirror; PD, photodetector; PZT, piezoelectric actuator; OI, optical isolator; VA, variable attenuator. Inset: (black curve) typical temporal evolution of an empty-cavity ring-down event as recorded by the detector $PD_1$, and (red curve) fitting of the experimental data to a single exponential decay.

 

than 1 h observation time was achieved by a 10 W Peltier cooler and a commercial temperature controller (Wavelength Electronic, Model PTC2.5K-CH). The QCL output beam is collimated to a diameter of 1.4 mm by an antireflection-coated aspheric lens glued onto the laser housing. The collimated light passing through a mode-matching lens, a beam splitter, and a variable attenuator is coupled to the V-shaped cavity. Build-up of the field occurs when the laser frequency matches the resonant modes of the cavity. The resonant OF is used to induce laser frequency self-locking to the top of a cavity $TEM_{00}$ resonance, resulting in a ideal single-frequency source. In practice, the frequency-filtered OF works as a frequency selected seed that narrows the laser emission linewidth well below the cavity mode width. The V-shaped resonator is made on a single Zerodur block, which assures high thermal stability (thermal expansion coefficient $\sim 10^{-7}$ $K^{-1}$). The resonator is 0.4 m long, resulting in an unfolded cavity length of 0.8 m, which, in turn, corresponds to a free spectral range (FSR) of about 187 MHz. The two cavity arms are set at an opening angle of about 4.4°. The optical cavity is obtained by directly gluing onto the Zerodur spacer three high-reflectivity plano–concave mirrors, made on a superpolished ZnSe substrate, with radius of curvature of 0.8 m and effective reflectance at 8.6 μm of 99.977% (LohnStar Optics). This latter was determined from the measurement of an empty cavity ring-down time of 5.8 μs (see the inset of Fig. 1), as recorded by a room-temperature amplified photodetector with 100 MHz bandwidth (Vigo, Model PVM-10.6-1x1). For a V-shaped geometry, this reflectance translates into a cavity finesse of ~6870, which, in turn, leads to a full width at half-maximum (FWHM) cavity mode of about 27 kHz. It is worth pointing out that, in vacuum conditions, the measured finesse corresponds to an effective optical path length of about 3 km. In an OF-cavity-based setup, the laser-to-cavity distance is a very critical parameter and it has to be carefully chosen and controlled to ensure the proper phase at the QCL for effective laser linewidth narrowing. For this purpose, mirror $M_{ph}$ in Fig. 1 has been mounted on a piezoelectric actuator (PZT) and used for a subwavelength-precise adjustment of the OF phase. Passive adjustment of the PZT voltage ensured the correct OF phase over several minutes. For longer times, an active adjustment of the optimum OF phase has to be implemented based on the first derivative detection of the cavity transmission by modulating the QCL injection current [15].

The OF-stabilized laser beam, available at the transmission of the beam splitter, passes through a custom 30 dB optical isolator (OI) [18] to reduce any detrimental contribution of unwanted parasitic optical feedback by other optical components. The relative intensity noise (RIN) of the OF-QCL was measured by analyzing the PSD of the photocurrent generated by a 200 MHz bandwidth mercury–cadium–tellurite sensor with a responsivity of $5.7 \times 10^4$ V/W and 50 nV/$\sqrt{\text{Hz}}$ noise floor at a temperature of 77 K (Kolmar, Model KV104-0.25-E1/KA200). Figure 2 depicts the RIN spectral density of the mid-IR radiation together with the photodetector noise floor. In the low Fourier frequency range, from 1 to 100 Hz, a low-pass behavior is observed (20 Hz cutoff), reducing the RIN from the 3 Hz value of −63 dB/Hz to the −101 dB level. After the peak at ~20 kHz, due

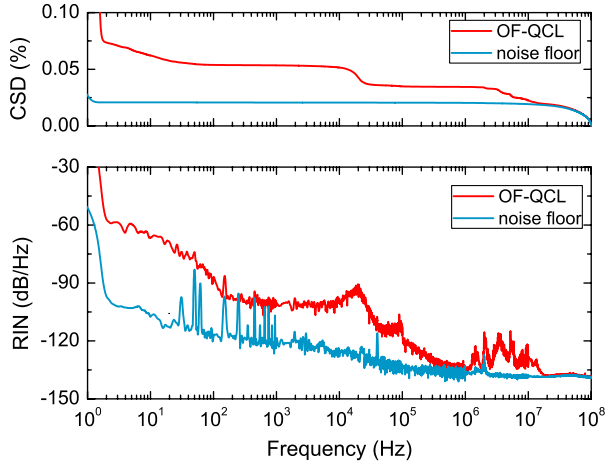


Fig. 2. RIN measurements of the OF-QCL: PSD (bottom chart) and cumulative standard deviation (top chart).

to technical noise in the current source, the RIN rapidly decreases, reaching the detector noise-floor level of −138 dB/Hz at frequencies larger than 20 MHz. The RIN level corresponding to the QCL pump current noise of the driver (Wavelength Electronic, Model QCL1500) is at a level of −144 dB/Hz for Fourier frequencies larger than 30 kHz. By numerical integration of the RIN spectrum, a cumulative standard deviation of the OF-QCL intensity lower than 0.1% over the range from 2 Hz to 100 MHz is obtained (see top chart in Fig. 2). It is worth noting that no significant differences are observed in the RIN measurements when the DFB-QCL operates in free-running condition, which is consistent with a Henry factor close to zero.

The QCL spectral purity was characterized in the frequency domain measuring the PSD of the frequency noise by means of two independent optical frequency discriminators. The first one exploits the side of a $N_2O$ absorption line to properly convert the laser frequency fluctuations into amplitude fluctuations. To this purpose, we used a 10 cm length cell filled with $N_2O$ gas at a pressure of 10 mbar. The measured transmission profile, corresponding the P(8) rotovibrational line of the $\nu_2$ vibrational band at 1161.479210 $cm^{-1}$ [19], is characterized by a FWHM of ~160 MHz, a maximum absorption of 86%, and a frequency-to-intensity conversion coefficient of 1.8 mV/MHz (corresponding to the slope of the transmission curve around the 0.8 V half-maximum point). The resulting frequency noise PSD of the QCL source, as measured by an electrical spectrum analyzer, is shown in Fig. 3(a) together with the RIN contribution (measured with an empty gas cell) and the detector noise floor (measured by obscuring the photodetector). In free-running, the QCL frequency noise is characterized by a flicker, $1/f$, contribution up to a Fourier frequency of 10 kHz, a result in good agreement with those previously published [1,2,6]. Then the PSD shows a bump at around 20 kHz, due to the QCL current noise as observed in the RIN spectrum, and a steeper slope ($\sim 1/f^2$) for Fourier frequency larger than 100 kHz. Figure 3(b) reports also the linewidth calculated from the measured PSD by means of the $\beta$-line method as introduced by [20], for different values of the integration bandwidth

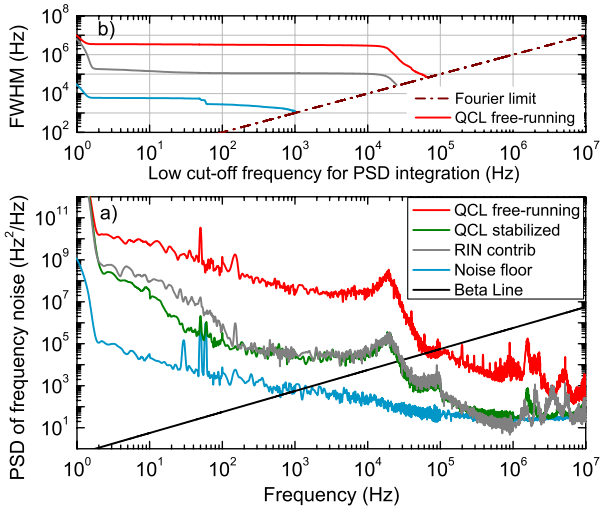


Fig. 3. (a) Frequency noise PSD of the QCL laser in free-running (red line) and in OF locking (green line) together with the RIN contribution (gray), the noise floor (blue), and the $\beta$-line, $8 \ln 2/\pi^2 f$ (black). (b) Calculated emission linewidth versus integration bandwidth.

(different observation times). In this way, a 1 ms emission linewidth of ~3.2 MHz is estimated.

When the OF from the V-shape cavity is activated, the PSD of the frequency noise cannot be measured using the gas discriminator, because its sensitivity is limited by the RIN contribution (see green and gray lines in Fig. 3). For this reason, a second optical frequency discriminator based on the fringe side of a high-finesse FP cavity with a FSR of 90 GHz (1.6 mm length) is used. Figure 4(a) shows the observed FP transmission when a scanning voltage is applied to the cavity PZT actuator. A good injection coupling of ~60% in the fundamental FP transverse mode is obtained, with a limited excitation of the higher-order transverse modes. A detailed view of the main FP fringe is reported in Figs. 4(b)–4(d) for the following conditions: (b) free-running QCL with OI, (c) OF-QCL without OI, and (d) OF-QCL with OI. In the first two cases, the FP fringes are strongly distorted by the laser frequency noise of the free-running QCL and by the parasitic self-injection of the OF-QCL by the FP resonance, respectively. The FP fringe becomes very symmetric [see Fig. 4(d)] when the optical isolator is used. In this case, a cavity linewidth of 6 MHz is measured (a finesse of ~15,000) with a maximum transmission of 1%. leading to an intensity conversion coefficient of 80 mV/MHz. The transmission signal is used to lock the low frequency jitter of the laser to the fringe midpoint through the PZT actuator of the FP interferometer (~100 Hz control bandwidth) and to measure the laser frequency fluctuations for Fourier frequency larger than the control bandwidth. Figure 5(a) shows the PSD of the OF-QCL frequency noise together with the measurement noise floor and the $\beta$-line. The PSD of the stabilized QCL reduces significantly with respect to the free-running QCL. In particular, the noise reduction factor reaches its maximum value of $\sim 10^9$ at 10 kHz Fourier frequency; for frequencies higher than 10 kHz, this factor initially decreases with a slope of –40 dB/dec and subsequently ($f > 100$ kHz) with a slope of –20 dB/dec, in fairly good agreement with the prediction of the theory in [11]. For frequencies lower than 10 kHz, a significant decrease of the noise reduction factor to $10^4$–$10^5$ values is observed, whereas the theory foresees a constant value of about $\sim 10^9$. This discrepancy is mainly ascribed to the measurement FP environmental noise. The PSD of the OF-QCL reaches a minimum noise floor at a level of $10^{-2}$Hz$^2$/Hz in the frequency range from 100 to 500 kHz and for frequencies larger than 5 MHz, corresponding to an intrinsic OF-QCL linewidth well below 1 Hz (assuming a white frequency noise contribution). According to [20], the frequency fluctuations above the beta separation line contribute to the central portion of the laser linewidth and, notably, to its linewidth, while the higher frequency noise ($f > 1.5$ kHz, i.e., the intersection point with the beta line) contributes only to the wings and pedestal. In Fig. 5(b), the calculated QCL linewidth is reported for different values of the integration bandwidth. For an

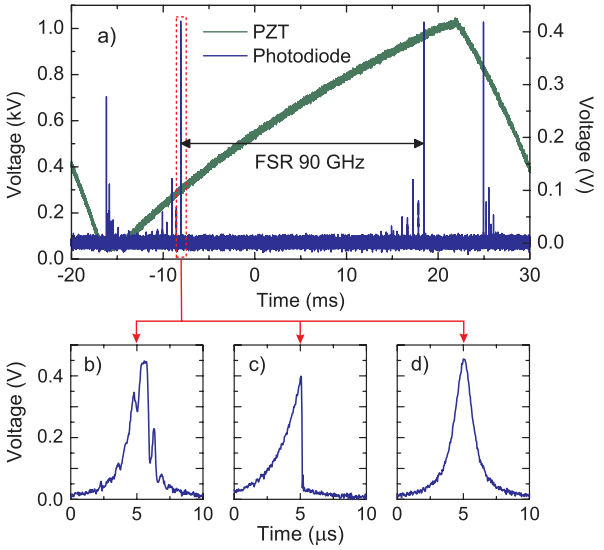


Fig. 4. (a) High-finesse FP transmission. Details of the fundamental FP fringe for (b) free-running QCL with OI, and for an OF-QCL (c) without and (d) with OI.

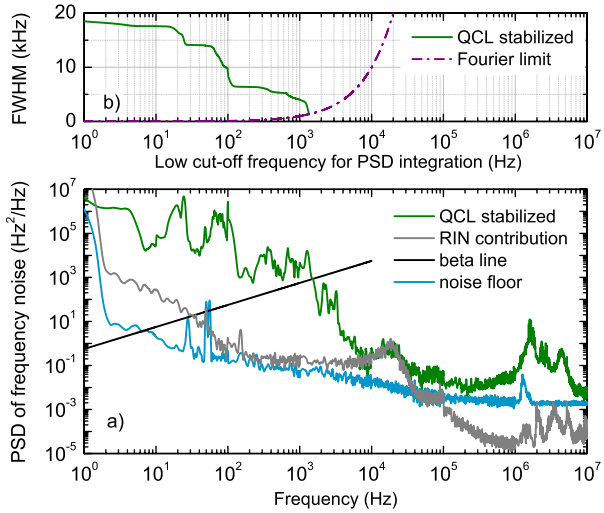


Fig. 5. (a) Frequency noise PSD of the OF-QCL laser (green line) together with the RIN contribution (gray), the noise floor (blue), and the $\beta$-line (black). (b) Calculated emission linewidth versus integration bandwidth.

observation time of 1 ms, a linewidth of 4 kHz is obtained, a factor 800 narrower than the free-running linewidth and even ~7 time narrower than the passive V-shaped cavity mode linewidth. It is worth pointing out that, for Fourier frequencies smaller than 1.5 kHz, the measured PSD of the frequency noise is mainly limited by the environmental noise acting on the 1.6 mm long FP resonator, leading to an overestimation of the OF-QCL linewidth for observation time longer than 0.6 ms. In fact, the same behavior and level of the PSD has been measured using an ultrahigh spectral purity Er-doped-fiber laser, replacing the mid-IR FP mirrors with a pair of high-reflection mirrors at 1.55 μm, keeping constant the cavity length.

In conclusion, we report on a high spectral purity room-temperature DFB-QCL in the wavelength range from 8.56 to 8.63 μm by means of the OF method on a high-finesse V-shaped cavity. An emission linewidth as narrow as 4 kHz is demonstrated over an observation time of 1 ms. Fine-tuning of the OF-QCL could be realized by using an external acousto-optic modulator in a double pass configuration, which should allow for continuous frequency shifting up to 1 GHz. This source will be a powerful tool for high-precision molecular spectroscopy and optical frequency standard in the mid-IR spectral region.

The authors acknowledge financial support from the Italian Ministry of University and Research, FIRB project no. RBFR1006TZ.

**References**

1. S. Bartalini, S. Borri, L. Galli, G. Giusfredi, D. Mazzotti, T. Edamura, N. Akikusa, M. Yamanishi, and P. De Natale, Opt. Express **19**, 17996 (2011).
2. L. Tombez, J. Di Francesco, S. Schilt, G. Di Domenico, J. Faist, P. Thomann, and D. Hofstetter, Opt. Lett. **36**, 3109 (2011).
3. L. Tombez, S. Schilt, J. Di Francesco, P. Thomann, and D. Hofstetter, Opt. Express **20**, 6851 (2012).
4. R. M. Williams, J. F. Kelly, J. S. Hartman, S. W. Sharpe, M. S. Taubman, J. L. Hall, F. Capasso, C. Gmachl, D. L. Sivco, J. N. Baillargeon, and A. Y. Cho, Opt. Lett. **24**, 1844 (1999).
5. M. S. Taubman, T. L. Myers, B. D. Cannon, and R. M. Williams, Spectrochim. Acta A **60**, 3457 (2004).
6. A. A. Mills, D. Gatti, J. Jiang, C. Mohr, W. Mefford, L. Gianfrani, M. Fermann, I. Hartl, and M. Marangoni, Opt. Lett. **37**, 4083 (2012).
7. F. Cappelli, I. Galli, S. Borri, G. Giusfredi, P. Cancio, D. Mazzotti, A. Montori, N. Akikusa, M. Yamanishi, S. Bartalini, and P. De Natale, Opt. Lett. **37**, 4811 (2012).
8. P. L. T. Sow, S. Mejri, S. K. Tokunaga, O. Lopez, A. Goncharov, B. Argence, C. Chardonnet, A. Amy-Klein, C. Daussy, and B. Darquié, Appl. Phys. Lett. **104**, 264101 (2014).
9. F. Bielsa, A. Douillet, T. Valenzuela, J. P. Karr, and L. Hilico, Opt. Lett. **32**, 1641 (2007).
10. B. Dahmani, L. Hollberg, and R. Drullinger, Opt. Lett. **12**, 876 (1987).
11. P. Laurent, A. Clairon, and C. Breant, IEEE J. Quantum Electron. **25**, 1131 (1989).
12. A. Hemmerich, D. H. McIntyre, C. Zimmermann, and T. W. Hansch, Opt. Lett. **15**, 372 (1990).
13. J. Morville, S. Kassi, M. Chenevier, and D. Romanini, Appl. Phys. B **80**, 1027 (2005).
14. G. Maisons, P. Gorrotxategi-Carbajo, M. Carras, and D. Romanini, Opt. Lett. **35**, 3607 (2010).
15. J. Burkart, D. Romanini, and S. Kassi, Opt. Lett. **38**, 2062 (2013).
16. L. Santamaria, V. Di Sarno, I. Ricciardi, S. Mosca, M. De Rosa, G. Santambrogio, P. Maddaloni, and P. De Natale, J. Mol. Spectrosc. **300**, 116 (2014).
17. P. Gorrotxategi-Carbajo, E. Fasci, I. Ventrillard, M. Carras, G. Maisons, and D. Romanini, Appl. Phys. B **110**, 309 (2013).
18. L. Hilico, A. Douillet, J. P. Karr, and E. Tournié, Rev. Sci. Instrum. **82**, 096106 (2011).
19. R. A. Toth, J. Opt. Soc. Am. B **3**, 1263 (1986).
20. G. Di Domenico, S. Schilt, and P. Thomann, Appl. Opt. **49**, 4801 (2010).